ChemPhysChem

Research Article
doi.org/10.1002/cphc.202300064

Chemistry Europe
European Chemical Societies Publishing

www.chemphyschem.org

Electron and Spin Delocalization in $[Co_6Se_8(PEt_3)_6]^{0/+1}$ Superatoms

Yunyao Xu,[a] Jia Chen,[a] Alexander P. Aydt,[a] Lichirui Zhang,[a] Ivan Sergeyev,[a] Eric G. Keeler,[a] Bonnie Choi,[a] Shoushou He,[a] David R. Reichman,[a] Richard A. Friesner,[a] Colin Nuckolls,[a] Michael L. Steigerwald,[a] Xavier Roy,*[a] and Ann E. McDermott*[a]

Molecular clusters can function as nanoscale atoms/superatoms, assembling into superatomic solids, a new class of solid-state materials with designable properties through modifications on superatoms. To explore possibilities on diversifying building blocks, here we thoroughly studied one representative superatom, $Co_6Se_8(PEt_3)_6$. We probed its structural, electronic, and magnetic properties and revealed its detailed electronic structure as valence electrons delocalize over inorganic $[Co_6Se_8]$ core while ligands function as an insulated shell. ^{59}Co SSNMR measurements on the core and ^{31}P, ^{13}C on the ligands show that the neutral $Co_6Se_8(PEt_3)_6$ is diamagnetic and symmetric, with all ligands magnetically equivalent. Quantum computations cross-validate NMR results and reveal degenerate delocalized HOMO orbitals, indicating aromaticity. Ligand substitution keeps the inorganic core nearly intact. After losing one electron, the unpaired electron in $[Co_6Se_8(PEt_3)_6]^{+1}$ is delocalized, causing paramagnetism and a delocalized electron spin. Notably, this feature of electron/spin delocalization over a large cluster is attractive for special single-electron devices.

Introduction

Here we elucidate the electronic structure of an atomically precise superatomic $[Co_6Se_8]$ cluster, highlighting its symmetry, stability and other electronic properties that are significant for its use as a building block in superatomic solids and single-electron devices. Metal chalcogenide clusters M_xE_y (where M is metal and E is chalcogenide), such as Mo_6E_8, Co_6E_8, Cr_6E_8, Ni_9E_6, have been discovered to interact with other clusters such as fullerenes through charge transfer to self-assemble into multi-component hierarchical structures, termed superatomic solids.[1–4] This observation opens the door to the design of unconventional solid-state materials with novel architectures and unique electronic, magnetic, and thermodynamic properties.[5,6] Future studies focus on expanding the pool of superatom candidates and modifying existing superatoms for desired properties. A study on structure-function relationship of these superatoms can provide a blueprint for these studies, allowing for tuning properties and driving new material applications.

The $Co_6Se_8(PEt_3)_6$ cluster has been used extensively as a superatom for assembling superatomic solids.[2,3] $Co_6Se_8(PEt_3)_6$ shares a similar structural motif with many other metal chalcogenide clusters, thus making it a suitable model cluster to study the structure-function relationship.[3,7] The availability of a large number of surface d orbitals makes it an interesting but complex cluster to study. Complications may come from different oxidation states of Co atoms that occurs in a potentially mixed-valence system, formation of metal-metal bonds, and possible Jahn-Teller effect that results in geometric distortion.[8–11] As a powerful tool to modify superatoms' properties,[12,13] ligand substitution modulates the HOMO-LUMO gap;[14,15] it could also introduce perturbations on the $[Co_6Se_8]$ inorganic core. Recent multi-wavelength anomalous diffraction studies on $Co_6Se_8(PEt_3)_5L$ (where L is CO or PBu_3) cluster reveals interesting ligand- and charge-dependent electron distribution over Co atoms: when L is a CO ligand, the attached Co is more oxidized than the other five Co atoms and the distribution is unchanged upon oxidation; when L is PBu_3 ligand, the six Co atoms are divided into two sets of three, each set being meridional, while they collapse into one environment upon oxidation.[16] Intriguing as these studies are, we lack a systematic model to thoroughly understand the inorganic core/ligands and associated properties, for which we need methods providing atomic resolution information to probe various sites within the clusters.

Solid-State NMR (SSNMR) is one of the few methods that provide structural, electronic, and magnetic information with atomic resolution, and it can provide a comprehensive view on both the core and the ligands as both the inorganic core atoms (^{59}Co, ^{77}Se) and ligand atoms (^{31}P, ^{13}C, ^{1}H) are NMR active. Owing to its versatility, SSNMR has been extensively applied to quantum dots,[17–19] metal-organic framework,[20–23] perovskites,[24–26] to obtain structural and electronic information.[27,28] Here, we present a multinuclear SSNMR study accompanied by Density-functionals Theory (DFT) calculations and Superconducting quantum interference device (SQUID) measurements to generate a molecular and electronic structure model for $Co_6Se_8(PEt_3)_6$. We start by elucidating the electronic symmetry of the cluster, by probing how many unique Co and

[a] Dr. Y. Xu, Dr. J. Chen, Dr. A. P. Aydt, L. Zhang, Dr. I. Sergeyev, Dr. E. G. Keeler, Dr. B. Choi, S. He, Prof. D. R. Reichman, Prof. R. A. Friesner, Prof. C. Nuckolls, Dr. M. L. Steigerwald, Prof. X. Roy, Prof. A. E. McDermott
Department of Chemistry
Columbia University
New York, New York 10027, USA
E-mail: xr2114@columbia.edu
aem5@columbia.edu

Supporting information for this article is available on the WWW under https://doi.org/10.1002/cphc.202300064

P environments in the cluster can be resolved. We have developed an electronic model for $Co_6Se_8(PEt_3)_6$ consistent with experimentally derived constraints on symmetry and magnetic properties of both the neutral and the cationic cluster $[Co_6Se_8(PEt_3)_6]^+[BF_4^-]$. This new model elucidates a number of functional properties of the clusters and provides many inspirations to tailor superatomic clusters for exciting applications, such as single-electron devices and tunable superatomic solids.

Results and Discussion

Delocalization and Symmetry of Electronic States in $Co_6Se_8(PEt_3)_6$

The electronic states of the $Co_6Se_8(PEt_3)_6$ clusters can be characterized in terms of the degree of delocalization of valence electrons. In one extreme, a valence-trapped situation would have distinct oxidation states for various Co atoms such as Co(II) or Co(III) (as in class I in the Robin-Day classification[29]). In another extreme, the states may be fully delocalized and/or symmetric so that the Co atoms are indistinguishable, (as in class III in the Robin-Day classification[29]) This distribution has implications for the molecular structure and properties. For example, the lengths of Co–P and Co–Se bonds are dependent on the oxidation state, which lead to different molecular structure geometry. For this example, given the stoichiometry and the fact that the cluster is charge-neutral, localized electronic states would cause paramagnetism and non-identical Co and Se and P sites in the cluster, *i.e.* low symmetry. Therefore, to understand the valence electron distribution, we investigated the structural symmetry of $Co_6Se_8(PEt_3)_6$, specifically the numbers of distinct atomic environments (*i.e.* ^{31}P, ^{59}Co) that can be detected using site-specific NMR chemical shifts.

A Symmetric Structure: ^{31}P NMR Reveals an Identical Environment for All Ligands

^{31}P NMR spectra of the PEt_3 ligands in $Co_6Se_8(PEt_3)_6$ cluster were obtained using Cross-Polarization Magic Angle Spinning (CPMAS) (Figure 1a). ^1H and ^{13}C spectra were also acquired, showing methylene and methyl peaks in ethyl group.(Figure S1, S2) The ^{31}P spectra consist of a center band (cb) and multiple spinning sidebands (ssb), the pattern of which reveals chemical shift anisotropy (CSA), which is intrinsically related to molecular orbitals and bonding.[30] Each peak (cb or ssb) is split into 8 J-coupled peaks due to the coupling of ^{31}P to the ^{59}Co nucleus (a quadrupole nucleus with spin $S=7/2$).[31] (Figure 1a,b, S3) Through spectral fitting using SIMPSON,[32] in which we included ^{31}P CSA, dipolar coupling and J-coupling between ^{31}P and ^{59}Co, ^{59}Co quadrupolar interaction, we show that the isotropic chemical shift is 64 ± 1 ppm, $^1J(^{59}Co,\ ^{31}P)$ is 665 ± 5 Hz, CSA values (in Haeberlen convention) are δ: -156 ± 4 ppm, η: 0.40 ± 0.05. (Figure 1a, Figure S4, Table S1) Notably, we observe only one ^{31}P chemical shift in the spectra, which, considering the narrow linewidth, indicates that there are no isomeric structures and all P atoms in the neutral cluster are in a very similar electronic environment. Narrow linewidths of NMR peaks suggest structural homogeneity and diamagnetism: static structural inhomogeneity (due to isomers, impurities or low symmetry) would cause inhomogeneous contributions to the linewidth, while paramagnetism would results in both homogenous or inhomogeneous broadening. The fitted linewidth (188 ± 43 Hz, Figures 1b and Figure S3) of the center band ^{31}P peak of $Co_6Se_8(PEt_3)_6$ indicates high homogeneity in the structure and electronic environment of neutral cluster and a diamagnetic core. The diamagnetism is further confirmed with nuclear spin-lattice relaxation T_1 measurements: $T_1(^{31}P)$ is 29 ± 3 s; $T_1(^{13}C$, methylene) is 2.8 ± 0.7 s; $T_1(^{13}C$, methyl) is 1.2 ± 0.2 s; $T_1(^1H)$ is 3.21 ± 0.04 s. (Figure 1e, Figure S5, S8). The T_1 values indicate that there is no paramagnetic center nearby the measured atoms. This diamagnetic property is further validated by SQUID measurement and temperature-independent shifts in NMR experiments (shown later). These NMR data indicate that all the P atoms in the cluster are chemically equivalent, suggesting that the directly bonded Co atoms are also equivalent. Together, these results point to a highly symmetric structure.

The high symmetry is consistent with the crystal structure, which can be best described as a face-capped octahedral (O_h) geometry (Figure 2a), with Co atoms in the center of cubic faces and Se atoms at the vertices of the cube.[1] We measured the bond-length of six Co–P bonds in the crystal structure and for its relaxed structure after quantum calculations; the Co–P bond-lengths in the relaxed structure are ~0.03 Å longer than experimental ones, but nonetheless all six bond-lengths are equivalent within the structure in both cases. (Table S2). As mentioned in the introduction, the multi-wavelength anomalous diffraction data reveal two sets of Co environments in $Co_6Se_8(PEt_3)_5(PBu_3)$.[16] The PBu_3 ligand is required in that study to break the structural symmetry so that different positions of Co atoms can be distinguished; however, PBu_3 has both different steric and electronic characteristics than PEt_3, which may introduce asymmetry in the core.

We also measured a CO-ligated analogous $Co_6Se_8(PEt_3)_5(CO)$ cluster (Figure 2b). By contrast, this compound shows broadened peaks in ^{31}P spectra (Figure 1c), with similar chemical shifts and CSA parameters ($\delta_{iso}=66\pm2$ ppm, δ: -154 ± 10 ppm, η: 0.44 ± 0.1) (Figure S9). Based on the spin lattice relaxation times ($T_1(^{31}P)$: 10.6 ± 0.2 s; $T_1(^{13}C$, methylene): 0.65 ± 0.08 s; $T_1(^{13}C$, methyl): 1.0 ± 0.2 s; $T_1(^1H)$: 2.35 ± 0.06 s.), $Co_6Se_8(PEt_3)_5(CO)$ is also a diamagnetic system (Figure 1e, Figure S6,S8). Likely the broadened linewidth is consistent with disorder in the P sites, due to the CO ligand breaking the symmetry. This is consistent with multi-wavelength anomalous diffraction results.[16] Similarly, we noticed the reduction in T_1 values, particularly in P atoms and C atoms in methylene group, which is probably caused by increased dynamics of the ligands due to a less ideal space-packing. The relatively small changes in ^{31}P chemical shift and CSA upon the CO ligand could be caused by the relatively subtle structural or electronic changes.

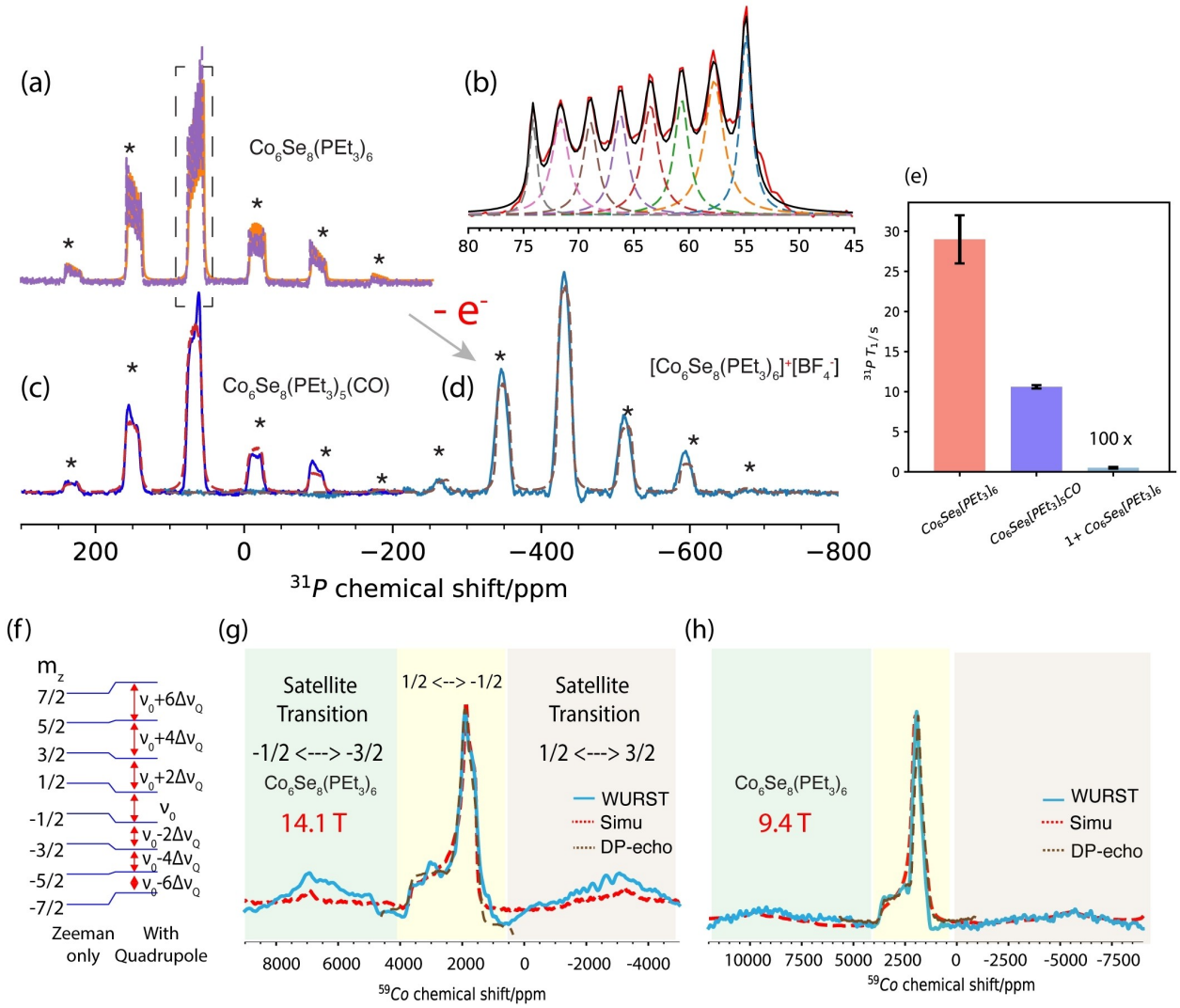

Figure 1. ^{31}P spectra (solid lines) and fitted spectra (dash lines) of a,b) $Co_6Se_8(PEt_3)_6$, c) $Co_6Se_8(PEt_3)_5(CO)$ and d) $[Co_6Se_8(PEt_3)_6][BF_4]$ clusters. Spinning sidebands are marked with asterisks (*). Fitting results (Table S1) indicate that Chemical shift Anisotropy (CSA) pattern is quite similar for all three compounds, despite the large changes in the isotropic chemical shift in $[Co_6Se_8(PEt_3)_6][BF_4]$ due to paramagnetic shift. The linewidth of the center band in $Co_6Se_8(PEt_3)_6$ is highlighted and fitted to 188 ± 43 Hz (b); linewidth in $Co_6Se_8(PEt_3)_5(CO)$ and $[Co_6Se_8(PEt_3)_6][BF_4]$ spectrum is much broader, likely due to structural heterogeneity and paramagnetism, respectively. e) ^{31}P spin-lattice relaxation T_1 values of three clusters (details in Figure S8); compared to the diamagnetic $Co_6Se_8(PEt_3)_6$ and $Co_6Se_8(PEt_3)_5(CO)$, the T_1 of paramagnetic $Co_6Se_8(PEt_3)_6][BF_4]$ is 3–4 orders of magnitude shorter. f) Energy diagram of a ^{59}Co (I = 7/2) nuclear spin in the presence of Zeeman interaction and quadrupolar interaction. g,h) WURST-QCPMG ^{59}Co spectra of $Co_6Se_8(PEt_3)_6$ taken at 14.1 and 9.4 T. It contains the central transition (1/2↔−1/2, yellow region) and satellite transitions (−1/2↔−2/3, green and 1/2↔2/3, tan). Both spectra were fitted (red dash lines); fitting values are compared to DFT-calculated values in Table 1. A hard pulse direct polarization with echo detection (brown dash line) was also applied to acquire ^{59}Co CT spectra to show consistency with the spectra taken with WURST-QCPMG.

A Symmetric Structure: ^{59}Co NMR Indicates One Environment for Co Atoms

^{59}Co NMR measurements are also consistent with the conclusion that the $Co_6Se_8(PEt_3)_6$ structure is highly symmetric. Quadrupolar nuclei, such as ^{59}Co, present particular challenges for NMR detection and the spectrum spans over a large chemical shift range due to their quadrupolar interactions together with chemical shift anisotropy.[33,34] We implemented WURST (Wideband Uniform Rate Smooth Truncation)-QCPMG (Quadrupolar Carr-Purcell Meiboom-Gill)[34] experiments to detect the ^{59}Co NMR signals of the neutral cluster, revealing a broad ^{59}Co spectrum (on the order of 10,000 ppm, Figures 1g–h). Spectra were recorded at two magnetic fields (9.4 T and 14.1 T). Both the central transition and the inner −1/2↔−2/3 and 1/2↔2/3 satellite transitions are detected in these experiments (Figure 1f); the singularities displayed in the satellite transitions are good for constraining of quadrupolar frequency. Side-by-side simulation of the spectra taken at two fields also restrains the determination of the spectral parameters, as the CSA interaction is linearly field dependent while the 2nd order quadrupolar interaction is inversely field dependent.(1st order quadrupolar interaction has no effect on CT in theory.)[35] The envelope of the central transition is dominated by the CSA interaction; best-fit parameters include an isotropic chemical shift of 2265 ± 50 ppm, and CSA values of δ_{11}: 3675 ± 100, δ_{22}: 1701 ± 100, δ_{33}:

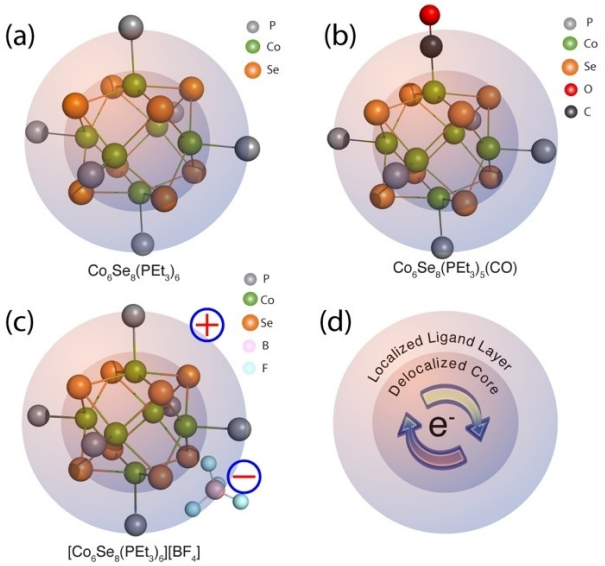

Figure 2. Crystal structures of a)$Co_6Se_8(PEt_3)_6$, b) $Co_6Se_8(PEt_3)_5(CO)$ and c) $[Co_6Se_8(PEt_3)_6][BF_4]$ as determined by SCXRD. The ethyl groups are removed for clarity. d) We hypothesize that these clusters contain an electron-delocalized inorganic core and an electron-localized ligand layer.

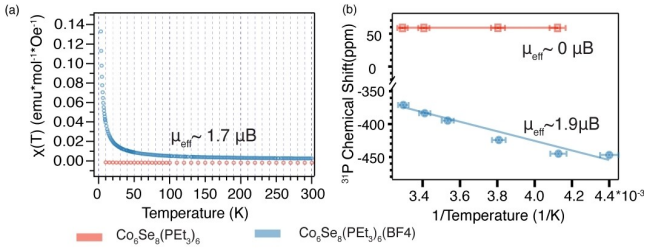

Figure 3. a) Magnetic susceptibility of $Co_6Se_8(PEt_3)_6$ (tomato) and $[Co_6Se_8(PEt_3)_6][BF_4]$ (blue) as a function of temperature. The data indicates that $Co_6Se_8(PEt_3)_6$ is diamagnetic and $[Co_6Se_8(PEt_3)_6][BF_4]]$ is paramagnetic. The data were fitted to Curie-Weiss law to derive effective magnetic moment for $[Co_6Se_8(PEt_3)_6][BF_4]$. The 1.7 μB value corresponds to ~1 unpaired electron. b) 31P chemical shift vs. 1/T for $Co_6Se_8(PEt_3)_6$ $[Co_6Se_8(PEt_3)_6][BF_4]$. The slopes of the linear fits are used to calculate the effect magnetic moment.

1419 ± 100 ppm (δ: 1410 ± 100 ppm, η: 0.20 ± 0.05). The quadrupolar coupling constant (C_Q) is 25 ± 2 MHz with an asymmetry parameter η_Q of 0.20 ± 0.05 (Table 1, Figure S11, S12); considering the quite large quadrupole moment ($Q = 0.42\times10^{-24}$ cm^2) for ^{59}Co, the C_Q and η_Q are consistent with a near symmetric Co environment, as was suggested also by the SCXRD. We also measured the CT spectra by using hard pulse direct polarization with echo (DP-echo) detection (Figure S13). The spectra are highly consistent with those taken by WURST-QCPMG (Figure 1 g–h, Figure S14). We estimated the effect of second-order cross term between Quadrupolar interaction and dipolar interaction on ^{31}P spectrum linewidth.[36](SI text) With C_Q at 25 ± 2 MHz, this second-order term is small compared to J-coupling, consistent with our observation of J-coupling resolved ^{31}P spectrum and narrow linewidth. To put these results in context, in Table S7, we survey the isotropic chemical shifts of a series of Co(III) and Co(I) compounds.[37–43] (NMR data for Co(II) are rare since Co(II) compounds are paramagnetic.) The isotropic chemical shift of $Co_6Se_8(PEt_3)_6$ has an intermediate value, suggesting that the ^{59}Co is in a delocalized system. (Figure S15).

The observation that $Co_6Se_8(PEt_3)_6$ is diamagnetic does not support the possibility that this system has a mixed-valence electronic configuration; if the system were Class I, the cluster would logically be expected to be paramagnetic since the Co(II) sites would have an odd-electron electronic configuration ([Ar]3d^7). The dephasing times (T_2*, revealed as narrow linewidths) for both ^{31}P and ^{59}Co, and longitude relaxation times (T_1), and magnetic susceptibility results (Figures 3a–b) indicate that $Co_6Se_8(PEt_3)_6$ is diamagnetic. Consistent with this argument, we could not acquire WURST-QCPMG ^{59}Co spectra for the 1+charged $[Co_6Se_8(PEt_3)_6][BF_4]$ cluster due to a short T_2*. The fast relaxation in T_2* is caused by paramagnetism, which is probed by ^{1}H, ^{13}C, ^{31}P T_1 measurements (Figure S7, S8), variable temperature NMR experiments and SQUID (Figures 3a–b) and is discussed later. We also acquired and fit ^{59}Co spectra for the $Co_6Se_8(PEt_3)_5(CO)$ cluster (Figure S16, S17, Table S6.) The ^{59}Co CSA do not significantly deviate from those of $Co_6Se_8(PEt_3)_6$, suggesting that electronic environment of P attached Co atoms predominately depends on local chemical bonding, but remotely affected through delocalization as the quadrupolar coupling constant is slightly reduced to 21 ± 2 MHz. This is likely due to the weaker electron-donating ability of CO ligand compared to phosphine ligands, reducing the overall electron density and rendering a smaller electron field gradient. We also observed another peak around 0 ppm, which has small CSA and C_Q(Difficult to quantify due to overlapped with ST signals from the major Co signal.) We tentatively assigned it to the CO attached Co atom. Further validation is needed for this assignment considering the big change in CSA and quadrupolar interaction.

To facilitate analysis of the ^{59}Co spectra, the NMR parameters derived above were compared to corresponding values calculated through DFT based on the crystal structure (Table 1). Analogous calculations were also performed for $Co(NH_3)_6Cl_3$ and $K_3Co(CN)_6$ and compared to experimental data to test the accuracy of these calculations (Tables S3, S4).[44,45] DFT based calculations for $Co_6Se_8(PEt_3)_6$ as well as the other compounds exhibited good agreement with the experimental results for these NMR parameters, including the isotropic chemical shift, its anisotropy, and asymmetry parameters, as well as the asymmetry of the EFG tensor. The calculated result on the quadrupolar coupling constant shows a noticeable ~30% deviation (Table 1). Considering the very challenging DFT calculations on the metal cluster, it is likely that the results are subject to computational errors, noting that we observe comparable deviations within this study for simpler complexes such as $Co(NH_3)_6Cl_3$ and $K_3Co(CN)_6$ and similar challenges are described in prior literature.[38,41]

Table 1. Experimental and DFT-calculated ^{59}Co NMR spectral parameters for $Co_6Se_8(PEt_3)_6$.

	δ_{11}/ppm	δ_{22}/ppm	δ_{33}/ppm	C_Q/MHz	η_Q	α/°C	β/°C	γ/°C
Exp.	3675 ± 100	1710 ± 100	1419 ± 100	25 ± 2	0.20 ± 0.05	32 ± 30	−8 ± 15	−30 ± 20
DFT[a]	3114 ± 75	1790 ± 60	1454 ± 230	33.8 ± 0.2	0.13 ± 0.01	−10 ± 30	−9 ± 20	−12 ± 30

[a] Averaged chemical shielding values for δ_{11}, δ_{22}, δ_{33} and Quadrupolar Coupling Constants (C_Q) and asymmetry η_Q are reported here for the six Cobalt sites. Reported errors of DFT calculation are from averaging values of the six sites; individual values are reported in Table S5.

DFT Calculation Reveals Delocalized HOMOs

The symmetry in the molecular structure as indicated by these NMR studies suggests that the electronic states (HOMO) may be delocalized. To further explore this hypothesis, we applied DFT calculation to investigate the electronic structure of $Co_6Se_8(PEt_3)_6$ by examining the HOMO and LUMO orbitals (Figures 4 a–d). The first two HOMOs (Figures 4a,b) are degenerate and their energy difference from HOMO level-1 (Figure 4c) is 0.02 eV (Figure 4e). These three pseudo-degenerate HOMOs are mainly made of the p-orbitals on the Se atoms. Consistent with X-ray and NMR results discussed above, the orbitals delocalize extensively and span the whole Co_6Se_8 core. In contrast, the P atoms in the PEt_3 ligands are likely isolated from the HOMOs since the electron density in the HOMOs do not extend to the P atoms (Figure 2d). The ^{31}P NMR also supports that the electron density in HOMOs resides mainly in the core, because the ^{31}P chemical shift and CSA are quite insensitive to the ligand change from PEt_3 to CO (Figure 1 and Table S1). These results imply that, by modifying their ligands, we can tune clusters for various purposes, such as solubility or dimensionality of the cluster-based material,[46] while leaving the electronic configuration in the core intact.[15,47] The ligand isolation of the delocalized core indicates that charge transfer in superatomic solid such as $Co_6Se_8(PEt_3)_6[C_{60}]_2$ is dominated by a charge hopping mechanism. Likewise, in a single molecule junction, the ligands isolate the leads from the cluster core to eliminate coherent tunneling, which renders cluster of this type ideal systems to study charge quantization in single molecule junction as current conducts by charging and discharging the cluster one electron a time.[48,49]

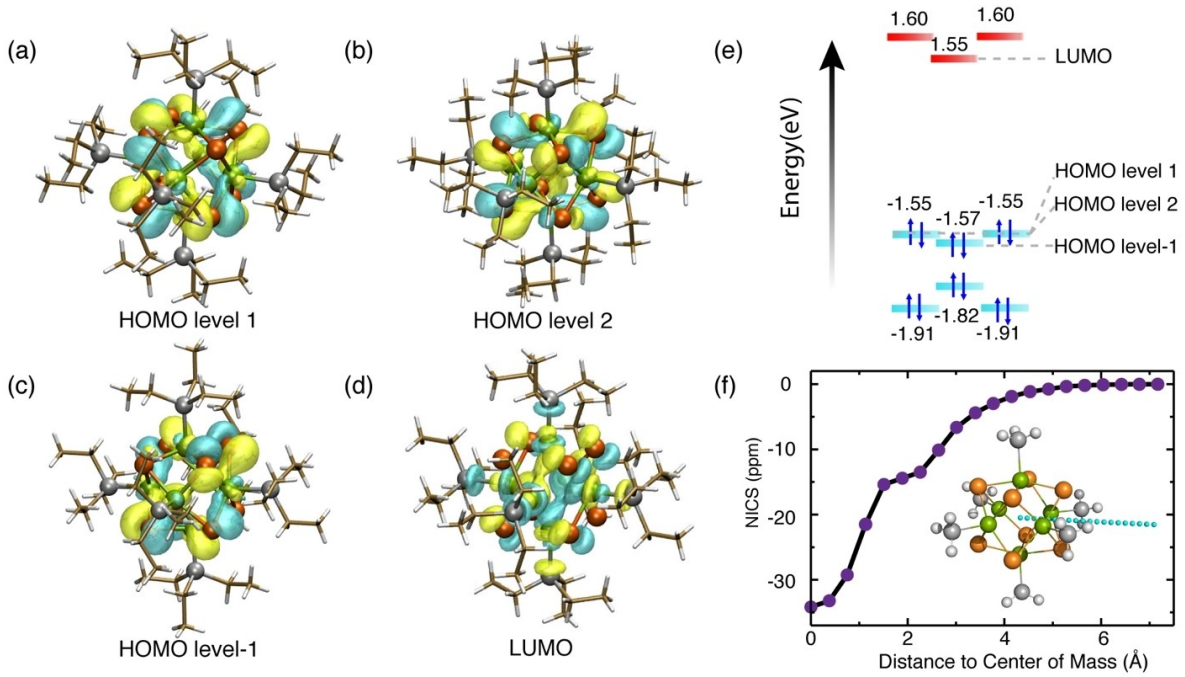

Figure 4. a–c) Iso-surfaces for the degenerate HOMO 1, HOMO 2 levels, and HOMO-1 level. The orbitals are delocalized over the core of the cluster. d) The iso-surface for LUMO orbital is delocalized on both the core and ligand P atoms. e) Energy diagram for the orbitals shown in (a–d). The first two HOMOs are degenerate. Once oxidized, the 1 + charge cluster has one delocalized hole. f) NICS values at as a function of distance for the center of mass of the cluster. NICS values were calculated for positions on the path (cyan dots) from the center to the outside of $Co_6Se_8(PH_3)_6$ cluster. The negative values indicate the aromatic property, generating ring-current and shielding the nuclei.

Ring Current on an Inorganic Core: An Aromatic Property

We hypothesized that the $Co_6Se_8(PEt_3)_6$ core could display aromatic like characteristics, in that the three delocalized HOMOs can provide mobile electrons that circulate to form ring-currents in magnetic fields.[50] Aromaticity has been demonstrated in inorganic and metallic molecules previously, for example Cu_4Li_2, Ga_3^{2-}, involving p-orbitals (i.e. π-aromaticity), s-orbitals (i.e. σ-aromaticity), or d-orbitals (i.e. δ-aromaticity).[51] We used a DFT-based method nucleus-independent chemical shifts (NICS)[51–54] to calculate the absolute chemical shielding on a virtual nucleus. A negative NICS value indicates an aromatic system and a positive value indicates an anti-aromatic system, while zero is non-aromatic.[51] NICS values were calculated for several positions from the center to the outside of this molecule (Figure 4f). At the center of Co_6Se_8 core, the NICS value is negative (suggesting an aromatic system[51]), and as the positions move to the outside of the core, NICS values gradually increase and eventually approach zero as the position moves away from the molecule. These results support our hypothesis of ring-current forming in the $Co_6Se_8(PEt_3)_6$ cluster, as a result of symmetric structure and degenerate delocalized HOMOs.

Ionized $Co_6Se_8(PEt_3)_6$ Is Also Symmetric

We tested whether the valence electrons are delocalized in the oxidized $[Co_6Se_8(PEt_3)_6][BF_4]$ form (Figure 2c). This 1+ charged cluster could be a proxy for $Co_6Se_8(PEt_3)_6$ in cluster-based solids, such as $[Co_6Se_8(PEt_3)_6][C_{60}]_2$, which undergoes electron transfer.[1,55] The ^{31}P spectrum is significantly shifted from 64 ppm to −430 ppm, presumably due to the cluster's paramagnetism, as well as change in cluster ring-current effect (Figure 1d). We observed similar upshift on methylene carbon (Figure S2). T_1 relaxation measurements on various nuclei ($T_1(^{31}P)$: 0.005 ± 0.001 s; $T_1(^{13}C$, methylene): 0.40 ± 0.02 s; $T_1(^{13}C$, methyl): 1.31 ± 0.04 s; $T_1(^1H)$: 0.254 ± 0.001 s.) shows that P atoms and methylene C atoms and proton atoms are influenced by a paramagnetic inorganic core (Figure S7, S8). ^{31}P spectrum linewidth is broadened due to paramagnetism so that the eight-peak splitting by ^{59}Co is no longer visible. Interestingly, we still observe mainly one P environment, even though subtle change of P environment may not be detected due to the broad linewidth. This indicates that loss of an electron does not obviously break the symmetry of structure. We attribute this to the stability of the delocalized electron configuration since the hole resides over the whole cluster and little structural reorganization is needed to accommodate the charge. Such a feature is presumably critical for $Co_6Se_8(PEt_3)_6$ to form superatomic solid with other clusters since the energetic penalty for reorganization after electron transfer is minimized.[56] In the spectra, we observed only small changes in central band and side bands pattern (Figure 1d, Figure S10). This pattern may also contain contributions from paramagnetic shift anisotropy besides CSA[57] but we assume that the influence is small due to the spherically-delocalized feature of the electron spin. It is worth noting that the significantly shifted ^{31}P chemical shift could be a particularly unique tool to identify charge-state of a cluster in study of cluster-based solids.

An Unpaired Electron/Spin Delocalized over the Whole Cluster Core

We contrasted the magnetic properties of neutral $Co_6Se_8(PEt_3)_6$ with the cationic $[Co_6Se_8(PEt_3)_6][BF_4]$ cluster. The magnetic properties of clusters have received tremendous attention;[58] here we aim to test whether our electronic structure model explains the cluster's magnetic properties. Figure 3a shows the magnetic susceptibility (χ) as a function of temperature for the neutral and 1+ cluster, as determined using SQUID magnetometry. Consistent with the NMR data, the neutral cluster is diamagnetic, as shown by the very small negative value for the susceptibility; in contrast, the 1+ charged cluster is paramagnetic, as shown by the positive values for the susceptibility. The magnetic susceptibility data was fitted with the modified Curie-Weiss law to acquire the effective magnetic moment (μ_{eff}) (Figure S18). The μ_{eff} of for $[Co_6Se_8(PEt_3)_6][BF_4]$ is close to 1.7 μ_B, consistent with ~1 unpaired electron, assuming spin-only contributions. A similar result ($\mu_{eff} = 1.9 \pm 0.1\ \mu_B$) is derived from the slope of chemical shift change over the temperature change using the Curie-Weiss equation (Figures 3b, Figure S19, Electron Spin calculation).[59] This is consistent with our electron-delocalized model: losing one electron causing one unpaired spin. Like the hole, the spin should be also delocalized as its influence on the ^{31}P chemical shift of the six ligands is almost the same, supported by our observation of only one P environment. To further test this idea, we did the Natural Population Analysis on both the neutral and the 1+ charged cluster; the results indicated that the natural charges on the 8 Se or 6 Co atoms remains equivalent for both clusters, confirming an electron delocalized configuration. The effect of losing an electron distributes to all inorganic core, making Se atoms less negative charged and Co/P atoms more positively charged and renders the 1+ cluster an unpaired spin. (Table S8, S9) Unlike an electron spin in an atom, the nature of a delocalized spin over a ~6 Å diameter core is of particular interest and may lead to potential interesting applications. With the features of quantized electron charge-discharge, single spin configuration, plus its atomically precise composition, the cluster would be a great candidate for a single spin manipulation in spin-dependent transport devices.[60]

Conclusions

We studied the molecular and electronic structures of $Co_6Se_8(PEt_3)_6$ cluster in order to build structure-property relationships for its application in superatomic solids and single molecule devices. Distinguishing between delocalized and mixed-valence electronic models for $Co_6Se_8(PEt_3)_6$ is key to probing the electronic structure. We used $[Co_6Se_8]$

clusters as an initial system to develop approaches to distinguish oxidation state assignments. Combining NMR, DFT and magnetic properties measurements by SQUID, we demonstrated that the structure of the $Co_6Se_8(PEt_3)_6$ cluster is highly symmetric with one P and Co environment, implying an electron-delocalized electronic structure. Other data are also consistent with highly delocalized HOMO electrons in the Co_6Se_8 cluster core, while the PEt_3 ligands are outside of the delocalized orbitals in the Co_6Se_8 cluster, based on both NMR and DFT calculations. The delocalized and degenerate HOMOs for the core shown in DFT calculation leads to aromatic-like properties, confirmed by NICS calculations. Moreover, NMR and SQUID measurements show that the neutral $Co_6Se_8(PEt_3)_6$ cluster is diamagnetic while the $1+$ $[Co_6Se_8(PEt_3)_6][BF_4]$ cluster is paramagnetic with one unpaired electron. Approaches demonstrated in the present work provides a molecular basis to understand these metal chalcogenide clusters, and can be used to investigate cluster-based building blocks in more complex heterogeneous solids.

Supporting Information

The authors have cited additional references within the Supporting Information.[61–79]

Acknowledgements

Support for this research was provided by the Center for Precision Assembly of Quantum Materials, an NSF MRSEC (award number DMR-2011738), and Air Force Office of Scientific Research (award number FA9550-22-1-0389). X. R. and S. H. acknowledge support from the NSF CAREER award program (award number DMR-1751949) We also want to thank Dr. Raul Hernandez and Dr. Anouck Champsaur for providing the first $Co_6Se_8(PEt_3)_5CO$ sample.

Conflict of Interests

The authors declare no conflict of interest.

Data Availability Statement

The data that support the findings of this study are available from the corresponding author upon reasonable request.

Keywords: superatomic solid · spin/electron delocalization · SSNMR · cluster aromaticity · quantum calculations

[1] X. Roy, C.-H. C.-H. Lee, A. C. Crowther, C. L. Schenck, T. Besara, R. A. Lalancette, T. Siegrist, P. W. Stephens, L. E. Brus, P. Kim, M. L. Steigerwald, C. Nuckolls, *Science* **2013**, *341*, 157–160.
[2] E. A. Doud, A. Voevodin, T. J. Hochuli, A. M. Champsaur, C. Nuckolls, X. Roy, *Nat. Rev. Mater.* **2020**, *5*, 371–387.
[3] A. Pinkard, A. M. Champsaur, X. Roy, *Acc. Chem. Res.* **2018**, *51*, 919–929.
[4] V. Chauhan, S. Sahoo, S. N. Khanna, *J. Am. Chem. Soc.* **2016**, *138*, 1916–1921.
[5] W.-L. Ong, E. S. O'Brien, P. S. M. Dougherty, D. W. Paley, C. Fred Higgs III, A. J. H. McGaughey, J. A. Malen, X. Roy, *Nat. Mater.* **2017**, *16*, 83–88.
[6] J. Yang, B. Zhang, A. D. Christodoulides, Q. Xu, A. Zangiabadi, S. R. Peurifoy, C. K. McGinn, L. Dai, E. Meirzadeh, X. Roy, M. L. Steigerwald, I. Kymissis, J. A. Malen, C. Nuckolls, *J. Am. Chem. Soc.* **2019**, *141*, 10967–10971.
[7] S. M. Stuczynski, Y. U. Kwon, M. L. Steigerwald, *J. Organomet. Chem.* **1993**, *449*, 167–172.
[8] A. Walsh, A. A. Sokol, J. Buckeridge, D. O. Scanlon, C. R. A. Catlow, *Nat. Mater.* **2018**, *17*, 958–964.
[9] N. Daelman, M. Capdevila-Cortada, N. López, *Nat. Mater.* **2019**, *18*, 1215–1221.
[10] P. Karen, *Angew. Chem. Int. Ed.* **2015**, *54*, 4716–4726.
[11] J. A. Kephart, B. S. Mitchell, A. Chirila, K. J. Anderton, D. Rogers, W. Kaminsky, A. Velian, *J. Am. Chem. Soc.* **2020**, *141*, 19605–19610.
[12] R. Hernández Sánchez, S. L. Zheng, T. A. Betley, *J. Am. Chem. Soc.* **2015**, *137*, 11126–11143.
[13] B. E. Petel, R. L. Meyer, M. L. Maiola, W. W. Brennessel, A. M. Müller, E. M. Matson, *J. Am. Chem. Soc.* **2020**, *142*, 1049–1056.
[14] V. Chauhan, A. C. Reber, S. N. Khanna, *J. Am. Chem. Soc.* **2017**, *139*, 1871–1877.
[15] G. Liu, A. Pinkard, S. M. Ciborowski, V. Chauhan, Z. Zhu, A. P. Aydt, S. N. Khanna, X. Roy, K. H. Bowen, *Chem. Sci.* **2019**, *10*, 1760–1766.
[16] R. Hernández Sánchez, A. M. Champsaur, B. Choi, S. G. Wang, W. Bu, X. Roy, Y.-S. Chen, M. L. Steigerwald, C. Nuckolls, D. W. Paley, *Angew. Chem. Int. Ed.* **2018**, *57*, 13815–13820.
[17] L. Piveteau, T. C. Ong, A. J. Rossini, L. Emsley, C. Copéret, M. V. Kovalenko, *J. Am. Chem. Soc.* **2015**, *137*, 13964–13971.
[18] L. Piveteau, T. C. Ong, B. J. Walder, D. N. Dirin, D. Moscheni, B. Schneider, J. Bär, L. Protesescu, N. Masciocchi, A. Guagliardi, L. Emsley, C. Copéret, M. V. Kovalenko, *ACS Cent. Sci.* **2018**, *4*, 1113–1125.
[19] V. Ladizhansky, G. Hodes, S. Vega, *J. Phys. Chem. B* **1998**, *102*, 8505–8509.
[20] B. E. G. Lucier, S. Chen, Y. Huang, *Acc. Chem. Res.* **2018**, *51*, 319–330.
[21] X. Kong, H. Deng, F. Yan, J. Kim, J. A. Swisher, B. Smit, O. M. Yaghi, J. A. Reimer, *Science* **2013**, *341*, 882–5.
[22] V. J. Witherspoon, J. Xu, J. A. Reimer, *Chem. Rev.* **2018**, *118*, 10033–10048.
[23] T. Kobayashi, F. A. Perras, T. W. Goh, T. L. Metz, W. Huang, M. Pruski, *J. Phys. Chem. Lett.* **2016**, *7*, 2322–2327.
[24] Y. Chen, S. R. Smock, A. H. Flintgruber, F. A. Perras, R. L. Brutchey, A. J. Rossini, *J. Am. Chem. Soc.* **2020**, *142*, 6117–6127.
[25] D. J. Kubicki, D. Prochowicz, A. Hofstetter, S. M. Zakeeruddin, M. Grätzel, L. Emsley, *J. Am. Chem. Soc.* **2017**, *139*, 14173–14180.
[26] G. M. Bernard, R. E. Wasylishen, C. I. Ratcliffe, V. Terskikh, Q. Wu, J. M. Buriak, T. Hauger, *J. Phys. Chem. A* **2018**, *122*, 1560–1573.
[27] M. Janssen, H. Eckert, W. Müller-Warmuth, U. Stege, R. Schöllhorn, *Chem. Mater.* **1998**, *10*, 3459–3466.
[28] Z. Jin, Q. Cheng, S. Tong Bao, R. Zhang, A. M. Evans, F. Ng, Y. Xu, M. L. Steigerwald, A. E. McDermott, Y. Yang, C. Nuckolls, *J. Am. Chem. Soc.* **2022**, *144*, 13973–13980.
[29] M. B. Robin, P. Day, *Adv. Inorg. Chem. Radiochem.* **1968**, *10*, 247–422.
[30] C. P. Gordon, S. Shirase, K. Yamamoto, R. A. Andersen, O. Eisenstein, C. Copéret, *Proc. Natl. Acad. Sci. USA* **2018**, *115*, E5867–E5876.
[31] R. W. Schurko, R. E. Wasylishen, J. H. Nelson, *J. Phys. Chem.* **1996**, *100*, 8057–8060.
[32] M. Bak, J. T. Rasmussen, N. C. Nielsen, *J. Magn. Reson.* **2000**, *147*, 296–330.
[33] R. Bhattacharyya, L. Frydman, *J. Chem. Phys.* **2007**, *127*, .
[34] L. A. O'Dell, R. W. Schurko, *Chem. Phys. Lett.* **2008**, *464*, 97–102.
[35] J. J. Hirschinger, P. Granger, J. Rosé, *Solid-State 59Co NMR in Tetrahedral Clusters, J. Phys. Chem.* **1992**, *96*,4815–4820.
[36] S. E. Ashbrook, J. McManus, M. J. Thrippleton, S. Wimperis, *Prog. Nucl. Magn. Reson. Spectrosc.* **2009**, *55*, 160–181.
[37] K. J. Ooms, V. V. Terskikh, R. E. Wasylishen, *J. Am. Chem. Soc.* **2007**, *129*, 6704–6705.
[38] K. J. Ooms, G. M. Bernard, A. Kadziola, P. Kofod, R. E. Wasylishen, *Phys. Chem. Chem. Phys.* **2009**, *11*, 2690–2699.
[39] R. Siegel, J. Hirschinger, D. Carlier, S. Matar, M. Ménétrier, C. Delmas, *J. Phys. Chem. B* **2001**, *105*, 4166–4174.

[40] J. C. C. Chan, S. C. F. Au-Yeung, *Annu. Reports NMR Spectrosc.* **2000**, *41*, 1–54.
[41] P. Crewdson, D. L. Bryce, F. Rominger, P. Hofmann, *Angew. Chem. Int. Ed.* **2008**, *47*, 3454–3457.
[42] A. Medek, V. Frydman, L. Frydman, *J. Phys. Chem. B* **1997**, *101*, 8959–8966.
[43] K. M. N. N. Burgess, C. M. Widdifield, Y. Xu, C. Leroy, D. L. Bryce, *ChemPhysChem* **2018**, *19*, 227–236.
[44] J. C. C. Chan, S. C. F. Au-Yeung, *J. Phys. Chem. A* **1997**, *101*, 3637–3640.
[45] N. Godbout, E. Oldfield, *J. Am. Chem. Soc.* **1997**, *119*, 8065–8069.
[46] A. M. Champsaur, J. Yu, X. Roy, D. W. Paley, M. L. Steigerwald, C. Nuckolls, C. M. Bejger, *ACS Cent. Sci.* **2017**, *3*, 1050–1055.
[47] W. L. Ong, S. M. Rupich, D. V. Talapin, A. J. H. McGaughey, J. A. Malen, *Nat. Mater.* **2013**, *12*, 410–415.
[48] G. Lovat, B. Choi, D. W. Paley, M. L. Steigerwald, L. Venkataraman, X. Roy, *Nat. Nanotechnol.* **2017**, *12*, 1050–1054.
[49] S. Gunasekaran, D. A. Reed, D. W. Paley, A. K. Bartholomew, L. Venkataraman, M. L. Steigerwald, X. Roy, C. Nuckolls, *J. Am. Chem. Soc.* **2020**, *142*, 14924–14932.
[50] J. M. Mercero, A. I. Boldyrev, G. Merino, J. M. Ugalde, *Chem. Soc. Rev.* **2015**, *44*, 6519–6534.
[51] Z. Chen, C. S. Wannere, C. Corminboeuf, R. Puchta, P. V. R. Schleyer, *Chem. Rev.* **2005**, *105*, 3842.
[52] P. von R. Schleyer, C. Maerker, A. Dransfeld, H. Jiao, N. J. R. van Eikema Hommes, *J. Am. Chem. Soc.* **1996**, *118*, 6317–6318.
[53] N. Toriumi, A. Muranaka, E. Kayahara, S. Yamago, M. Uchiyama, *J. Am. Chem. Soc.* **2015**, *137*, 82–85.
[54] L. Alvarado-Soto, R. Ramírez-Tagle, R. Arratia-Pérez, *J. Phys. Chem. A* **2009**, *113*, 1671–1673.
[55] E. S. O'Brien, M. T. Trinh, R. L. Kann, J. Chen, G. A. Elbaz, A. Masurkar, T. L. Atallah, M. V. Paley, N. Patel, D. W. Paley, I. Kymissis, A. C. Crowther, A. J. Millis, D. R. Reichman, X.-Y. Zhu, X. Roy, *Nat. Chem.* **2017**, *9*, 1170–1174.
[56] H. Tributsch, L. Pohlmann, *Science.* **1998**, *279*, 1891–1895.
[57] B. J. Walder, K. K. Dey, M. C. Davis, J. H. Baltisberger, P. J. Grandinetti, *J. Chem. Phys.* **2015**, *142*, 14201.
[58] C. J. Milios, R. E. P. Winpenny, *Cluster-BasedSingle-Molecule Magnets* Springer Berlin Heidelberg, Berlin, Heidelberg, **2015**, lpp. 1–109.
[59] I. Heinmaa, S. Vija, E. Lippmaa, *Chem. Phys. Lett.* **2000**, *327*, 131–136.
[60] J. Martinek, J. Barnaś, *in Concepts in Spin Electronics.*(Ed.: S. Maekawa), Oxford University Press, **2007**, l pp. 1–45.
[61] F. H. Larsen, H. J. Jakobsen, P. D. Ellis, N. C. Nielsen, †Flemming H. Larsen, †Hans J. Jakobsen, Paul D. Ellis, †Niels Chr. Nielsen*, F. H. Larsen, H. J. Jakobsen, P. D. Ellis, N. Chr Nielsen, N. C. Nielsen, *J. Phys. Chem. A.* **1997**, *101*, 8597–8606.
[62] R. K. Harris, E. D. Becker, S. M. Cabral De Menezes, P. Granger, R. E. Hoffman, K. W. Zilm, *Solid State Nucl. Magn. Reson.* **2008**, *33*, 41–56.
[63] J. J. Helmus, C. P. Jaroniec, *J. Biomol. NMR* **2013**, *55*, 355–367.
[64] V. K. Michaelis, E. G. Keeler, T. C. Ong, K. N. Craigen, S. Penzel, J. E. C. Wren, S. Kroeker, R. G. Griffin, *J. Phys. Chem. B* **2015**, *119*, 8024–8036.
[65] P. J. Stephens, F. J. Devlin, C. F. Chabalowski, M. J. Frisch, *J. Phys. Chem.* **1994**, *98*, 11623–11627.
[66] B. Miehlich, A. Savin, H. Stoll, H. Preuss, *Chem. Phys. Lett.* **1989**, *157*, 200–206.
[67] F. Neese, *WIREs Comput. Mol. Sci.* **2018**, *8*, e1327–e1327.
[68] X. Roy, C. L. Schenck, S. Ahn, R. A. Lalancette, L. Venkataraman, C. Nuckolls, M. L. Steigerwald, *Angew. Chem. Int. Ed.* **2012**, *51*, 12473–12476.
[69] T. Helgaker, M. Jaszuński, K. Ruud, *Chem. Rev.* **1999**, *99*, 293–352.
[70] R. Ditchfield, *Mol. Phys.* **1974**, *27*, 789–807.
[71] F. London, *J. Phys. Radium* **1937**, *8*, 397–409.
[72] S. Koseki, M. W. Schmidt, M. S. Gordon, *J. Phys. Chem. A* **1998**, *102*, 10430–10435.
[73] S. Koseki, M. S. Gordon, M. W. Schmidt, N. Matsunaga, *J. Phys. Chem.* **1995**, *99*, 12764–12772.
[74] C. Cao, J. L. Chen, Y. Yang, F. Huang, G. Otting, X. C. Su, *J. Biomol. NMR* **2014**, *59*, 251–261.
[75] Q. Sun, T. C. Berkelbach, N. S. Blunt, G. H. Booth, S. Guo, Z. Li, J. Liu, J. D. McClain, E. R. Sayfutyarova, S. Sharma, S. Wouters, G. K. L. Chan, *WIREs Comput. Mol. Sci.* **2018**, *8*: e1340.
[76] "NMR Ramblings Klaus Eichele," can be found under http://anorganik.uniuebingen.de/klaus/nmr/index.php?p=conventions/csa/csa.
[77] P. Zhou, S. C. F. Au-Yeung, X. P. Xu, *J. Am. Chem. Soc.* **1999**, *121*, 1030–1036.
[78] T. Pathmalingam, F. Habib, C. M. Widdifield, F. Loiseau, T. J. Burchell, S. I. Gorelsky, A. M. Beauchemin, D. L. Bryce, M. Murugesu, K. R. Dunbar, *Dalton Trans.* **2010**, *39*, 1504–1510.
[79] A. Medek, V. Frydman, L. Frydman, *Proc. Natl. Acad. Sci. USA* **1997**, *94*, 14237–14242.

Manuscript received: January 24, 2023
Revised manuscript received: November 1, 2023
Version of record online: December 6, 2023